ICSO 2016

International Conference on Space Optics

Biarritz, France

18–21 October 2016

Design study for an active metal mirror: sub-system of a correction chain for large UVOIR space telescopes

M. Goy

C. Reinlein

N. Devaney

A. Goncharov

et al.

DESIGN STUDY FOR AN ACTIVE METAL MIRROR: SUB-SYSEM OF A CORRECTION CHAIN FOR LARGE UVOIR SPACE TELESCOPES

M. Goy[1,2], C. Reinlein[1], N. Devaney[3], A. Goncharov[3], R. Eberhardt[1], A. Tünnermann[1]

[1]*Fraunhofer Institute for Applied Optics and Precision Engineering IOF, Albert-Einstein-Str. 7, D-07745, Jena, Germany*

[2]*Institute of Applied Physics, Abbe Center of Photonics, Friedrich Schiller University Jena, Max-Wien-Platz 1, 07743 Jena, Germany*

[3]*School of Physics, National University of Ireland, Galway, Ireland*

I. INTRODUCTION

Large UVOIR (ultraviolet-optical-infrared) space telescopes that are going to be designed within the next decades are intended to answer the question about life on exoplanets [1], [2]. Those systems will demonstrate a huge leap in optical quality and scientific advancement compared to the Hubble Space Telescope (HST). Otherwise, there is no reason to start such cost-intensive projects. The most effective way to identify more Earth-like planets is to enlarge the primary mirror to 4, 8, 12 or 16 meters. However, in doing so, the aspect ratio of the primary mirror will increase and hence suffer drastically from gravity release after reaching space surface distortions due to thermal changes and vibrations. Large aperture monolithic optics must be designed as lightweight components to reduce launch costs. Hence, misalignment of these components and inherent manufacturing caused surface errors must be taken into account as well. Optical aberrations due to those unavoidable effects could be corrected by an active optics correction chain [3]. In this case does not require high dynamic as it is mandatory for the correction of atmospheric turbulence, but an excellent long-term stability in wave front control.

The main idea of the paper is to show the developing process from the application requirements to the preliminary design of an active metal mirror as an essential sub-system of the telescope structure. All investigations are performed within the STOIC (Space Telescope Optical Image Corrector) project in response to an ESA invitation to develop an active optics correction chain for future space telescopes. The baseline space telescope (HYPATIA) being considered in this study, is a Ritchey-Chrétien-Cassegrain-telescope with a 4 m monolithic primary mirror [3]. The active mirror has to be designed for high precision and the ability to maintain a stable shape over long periods of time. As the space telescope will be located in L2 where the environmental conditions are harsh and energy is rare, a reliable set-and-forget approach with "powerless" actuators is implemented. 'Set-and-forget'-DMs for Earth based applications were investigated previously by [4], [5], [6] and [7]. The principal of the HYPATIA correction chain is to separate the modes of aberration that has to be corrected into low and high order. Low order aberrations such as misalignment perpendicular to the optical axis, tip/tilt and defocus are corrected by the displacement of the secondary mirror. The deformable mirror whose development process is being shown in this paper addresses higher order aberrations. The DM is positioned conjugate to the primary mirror. Its shape is concave with a radius of about 2 m.

In the first part of the paper we present a simulation tool for determining an appropriate actuator layout for the deformable mirror which meets the given requirements depending on the number of actuators, their distribution, the shape of the deformation and the optical aperture. With the help of a simplified finite element model we analyze the shape of the actuator influence function (AIF) depending on the stiffness of the mirror support and what residual error we can achieve using this AIF. The second part of the paper is describing the conceptual design as well as the manufacturing process we will use to assemble a demonstrator.

II. DEFINITION OF ACTUATOR LAYOUT

As a first step, the definition of the actuator layout was done by the use of a MATLAB tool which allows the evaluation of several actuator distributions (grids), shapes of actuator influence functions and active optical apertures. Those parameters were varied to find an actuator layout which meets the given requirements. The most promising layout was used to setup a model that will be refined in a subsequent FE analysis.

A. Requirements for the deformable mirror's optical performance

The deformable mirror which is intended for operation within the UVOIR wavelength range (0.1 - 2 µm) must mandatory have high quality optical surface. The deviation from the desired shape (sphere) should be lower than 15 nm rms. The overall Zernike mode reproduction should be done with an accuracy of 20 nm rms and ~5 nm rms per mode. Tab. 1 shows the required Zernike modes that should be corrected by the deformable mirror. As

Tip/Tilt (and defocus are covered by a displacement of the secondary mirror of the telescope, the modes that should be corrected by the deformable mirror start with Astigmatism (mode number 5). The RMS-values for the individual modes were specified individually by ESA, where coma and astigmatism represents the highest. The amplitudes for each mode are calculated by the use of an appropriate transformation factor.

Tab. 1. RMS and amplitude values of the Zernike modes that have to be corrected (Noll index).

Mode number	Zernike Mode name	RMS [nm]	Amplitude [nm] (calculated)
05	Astigmatismus 3x	200	545.93
06	Astigmatismus 3y	200	550.46
07	Coma 3x	300	950.40
08	Coma 3y	300	950.40
09	Sphere 3	75	190.71
10	Trifoil 5x	50	159.93
11	Trifoil 5y	50	159.93
12	Astigmatismus 5x	50	172.10
13	Astigmatismus 5y	50	175.14
17	Tetrafoil 7x	50	176.42
18	Tetrafoil 7y	50	178.49
19	Trifoil 7x	50	195.74
20	Trifoil 7y	50	195.74
26	Pentafoil 9x	50	195.17
27	Pentafoil 9y	50	195.17
28	Tetrafoil 9x	50	196.60
29	Tetrafoil 9y	50	210.19

B. MATLAB-Tool

All Zernike modes that are listed in Table 1 have to be reproduced with high accuracy. A MATLAB script was used to evaluate and improve several actuator distributions (grids) as well as the shapes of the actuator influence function. That Zernike mode that has to be reproduced is set as the *input wave front*. Furthermore, the number of actuators n, the shape (circular/rectangular) of the mirror substrate, the clear aperture d and an extended diameter d_{ext} of the mirror must be defined. The shape of the actuator influence function is approximated by a Gaussian profile. The width w, which is defined as the 1/e² width, is a multiple of the actuator distance of the used actuator grid. All parameters that are defined here are normalized to the diameter d of the mirror substrate. Fig. 1 shows a graphical representation of the parameters.
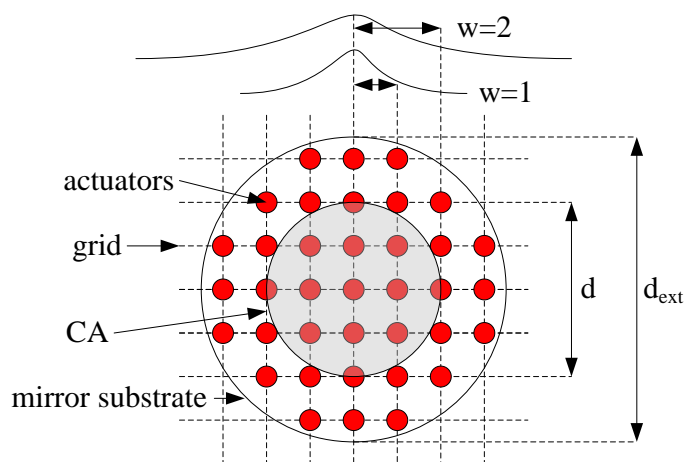

Fig. 1. Graphical presentation of the definable parameters for the best fit method to recreate the wave fronts

Fig. 2 shows the five grid variants that we have considered in the simulations. We determined the residual wavefront error for each specified Zernike mode for a range of different numbers n of actuators, grid type, extended diameter and the width of the AIF.

All residual errors from each Zernike mode are summed up and result in the overall RMS deviation. This value is used as a baseline to compare the individual parameter sets. The results are shown in Fig. 3 for all Zernike modes. The residual RMS is shown as a function of the number of actuators where the different curves represent the different grid variants.
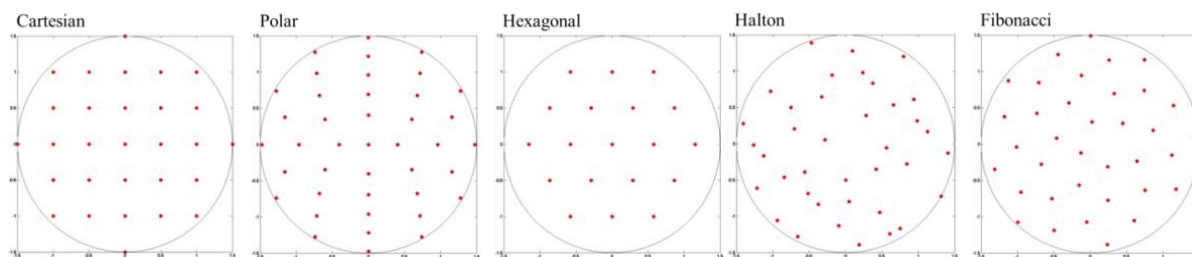

Fig. 2. Distribution of 36 actuators for the five analysed grid variants. The substrate is extended by the factor of 1.5 with respect to the diameter of the mirror surface. The red dots show the centers of the actuator influence functions
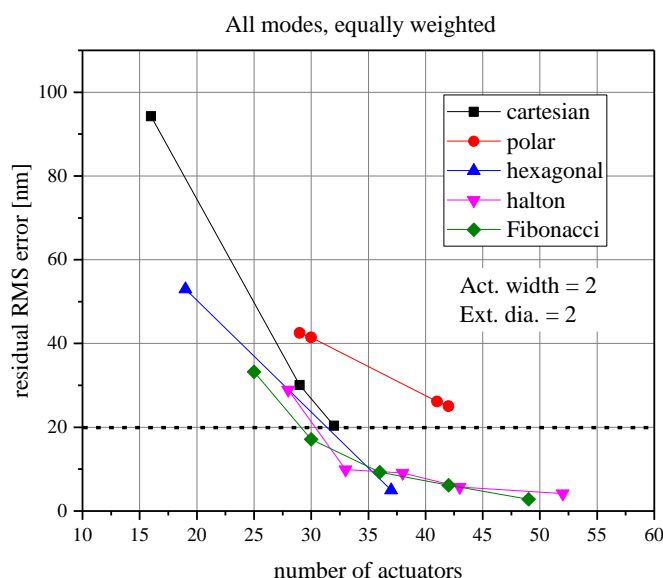

Fig. 3. The residual RMS error obtained by summing the residual RMS error of the individual Zernike modes as a function of the number of actuators for different actuator geometries

All simulation shown here was done with an AIF width of 2 and an extended diameter of 2 (see Fig. 1). As can be seen, a Cartesian or polar actuator distribution is not suitable for the correction of the desired Zernike modes within the error range of 20 nm RMS. The residual RMS error for the sum of all Zernike modes reaches 94 nm in the worst case (Cartesian). The curve with the circular data points indicates that only a high number of actuators and a polar grid can reach the specified wave front error of 20 nm. In contrast, it is noticeable that the other grid variants (Hexagonal, Halton and Fibonacci) can achieve much lower RMS values also with lower numbers of actuators. The hexagonal grid is restricted with regard to the number of actuators as only 1, 7, 19, 37 and 61 actuators (adding a hole ring) are allowed in this arrangement. The simulations show that only 37 or more actuators can reach the requirements. Better results were found with a Halton or Fibonacci grid, whereas the actuator distance of the Halton grid is problematical. Some actuators are spaced close together and make the manufacturing more or less impossible. The lowest values are reached for parameter sets with a wide AIF (factor of 3 and 5) and for a high number of actuators, well above 42. Therefore, the optimum of a low number of actuators and a low residual wavefront error can be found for either a hexagonal or a Fibonacci grid based actuator distribution with 36 actuators for a wide AIF. Both a hexagonal and a Fibonacci distribution with 37 or

36 actuators and an extended diameter factor of between 1 and 2 are considered suitable for the application. It could be proven that a large AIF width can reduce the residual error drastically. Values about 3 nm RMS could be reached. This analysis is based on ideal Gaussian profiles for the actuator influence function. However, real deformations that are generated by the stroke of the actuators may be different. A subsequent finite element analysis will be used to accurately predict the actuator influence functions for a final assessment of the residual error.

C. Simplified FE model

A simplified FE model was introduced to investigate the influence of the stiffness of the support structure on the deflection characteristics of the mirror substrate. A certain stiffness is required to reproduce a desired AIF shape (AIF width) that ensures low residual errors within the Zernike mode reproduction. As a first step, we developed a simple model as shown in Fig. 4. A circular mirror substrate is equipped with equidistant arranged coupling points (221 pc.) in a Cartesian grid. The substrate (AlSi-composite, Young's modulus: 107 GPa) has a diameter of 500 mm and a thickness of 3 mm. All coupling points are supported elastically by spring elements. Those elements are replacing the stiffness of all components that are used for the mirror deformation i.e. the actuators, and transmissions that include a spring for the pretension of the actuators. The large number of coupling points was used to avoid a significant influence of the substrate rim.
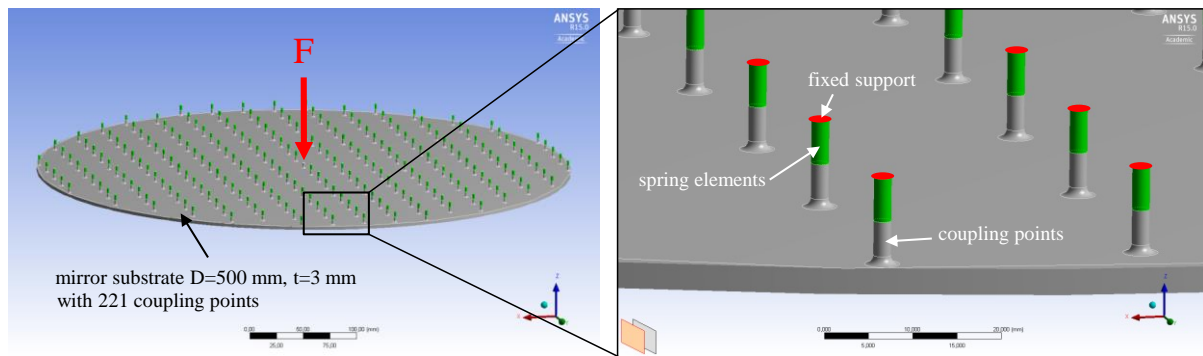

Fig. 4. Simplified FE-model. It consists of the mirror substrate, coupling points and spring elements

Within a parameter study, where the stiffness of each spring element is varied, we determined its influence on the width of the actuator influence function (AIF). From our preliminary analytical investigation, we found AIF widths between 2 and 5 favourable.

As can be seen in the chart (Fig.5, left), a stiffness of about 1000 N/mm leads to an AIF width of 2 – an AIF width of 3.5 will be reached with a stiffness of about 90 N/mm. Please noticed, that the stiffness of the substrate itself is defined by the material and the thickness which remain constant in the analysis. However, the smallest spring stiffness is somewhat equivalent to a simple support, whereas a high stiffness approximate a fixed support. If thickness or material will change, the shape of the AIF will change as well. The calculation of the support stiffness has to be repeated.
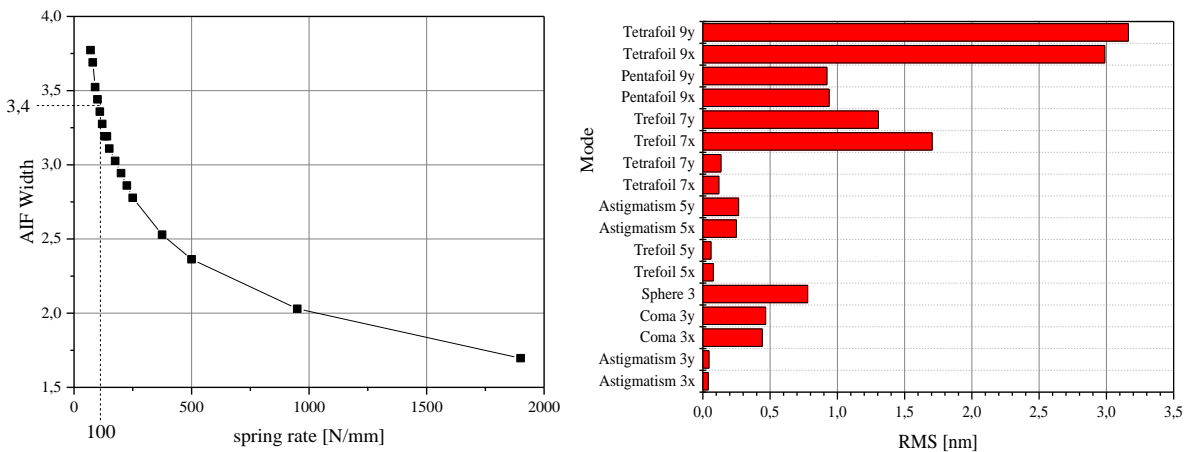

Fig. 5. Left: Width of the actuator influence function depending on the stiffness of the mirror support. Right: Residual RMS error of the desired Zernike modes with an AIF width of 3.4

In the next step, we used the numerical results within the MALAB-tool to simulate the accuracy of Zernike mode reproduction for one actuator layout:

- 36 actuators
- Fibonacci distribution
- clear aperture = 110 mm
- extended diameter=220 mm

The spring rate was fixed to 100 N/mm achieving an AIF width of 3.4. Then the AIF are scaled to match the residual Zernike modes while the residual errors are sampled. The right side of Fig. 5 depicts the results of the analysis. Except from both orientations of the Tetrafoil9 mode all modes can be reproduced with a very low residual error, lower than 2 nm RMS. The summed residual RMS is 3.7 nm. This result is remarkable as by only changing the AIF with, the summed residual error is reduced by a factor of 2 compared to an AIF width of 2.

D. DEVELOPMENT OF THE ENTIRE SIMULATION ROUTINE

After a rough analysis of our simplified FE model a refined model with the desired Fibonacci actuator distribution has to developed. Fig. 6 shows the entire scheme of simulations that will be done within the design phase of this project.
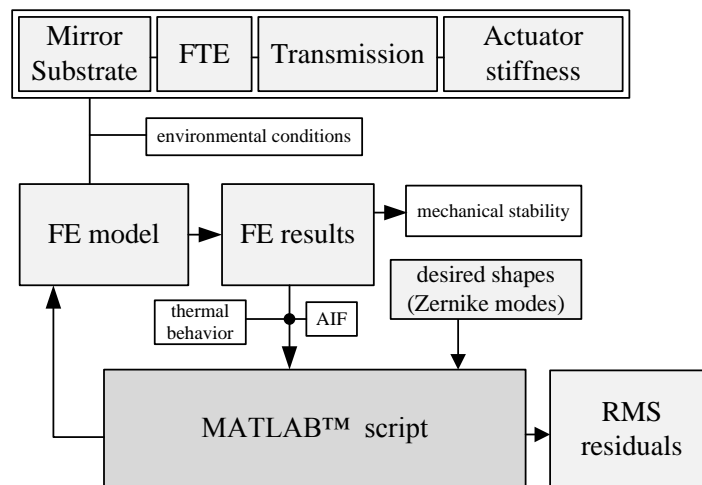

Fig. 6. Development routine of the DM design process

The mirror substrate, the coupling points (FTE), the transmissions and the actuator stiffness are the elements that will be combined in the refined FE model. Environmental conditions, such as gravity, temperature changes and acceleration, as well as the actuator force, will be set as boundaries or external loads. The result of one simulation is the deformation of the mirror surface known, as the actuator influence function. This AIF is now closer to reality than the Gaussian assumption we have made in the previous MATLAB calculation. The AIF and the desired Zernike modes act as input for the final MATLAB calculation which will result in the final RMS residuals. Final results of this optimization will provide the base for the realization of the conceptual or preliminary design.

III. CONCEPTUAL DESIGN

The content of this section will be the conceptual design of the DM. This includes a discussion of the requirements, the mechanical concept and the manufacturing process that could be derived.

A. Requirements for the opto-mechanical design of the deformable mirror

Like for every opto-mechanical component or system that has to operate in space, the requirements are demanding. Except from the high optical quality, which has to be ensured for operation, the non-operational requirements are challenging as well. The DM should work in vacuum environment and has to maintain its optical surface figure within a temperature change of ±2 K over a period of one month – without energy. This means, a 'set-and-forget' solution is indispensable in that case.

B. DM concept

The deformable mirror which shall be realized as a semi-monolithic design consists of the mirror body that is separated into two components – the base plate and a cup-shaped mirror substrate. Both components are made from the same AlSi-composite. 36 actuators that are integrated in the base plate provide force perpendicular to the mirror substrate. The clear aperture (CA) of this concept is given by the optical design of the telescope and is set to 110 mm. The entire diameter of the deformable mirror will be approximately 250 mm. This is caused by the extended diameter of 2, and the surrounding mechanics. 17 of the 36 actuators will be located outside the CA. They will cause deformations inside but with lower amplitude than those actuators located inside. This way, a much smoother surface deformation can be realized, especially at the rim of the CA.
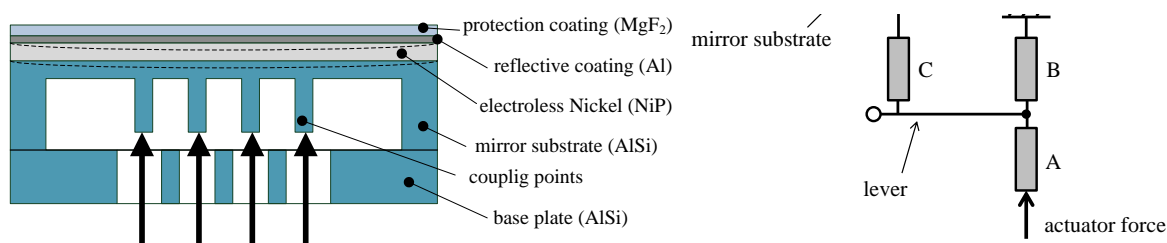

Fig. 7. Left: Semi-monolithical concept for the deformable mirror, Right: equivalent circuit of the transmission elements

Maintaining the shape of the mirror surface without power over a period of one month is the most important of the non-operational requirements. Therefore we have chosen very high accuracy actuators which provide self-locking ability. Transmission elements between the actuators and the coupling points are implemented to reduce the displacement of the actuators and hence their step size, and increase the force that is provided by each actuator. These transmission elements work as levers, the equivalent circuit of which is illustrated in Fig. 7. It consists of 3 spring elements. A is the elasticity of the actuator itself; B is a spring which ensures the pretension that is needed to preload the actuator and to realize 'negative' stroke. C is the elasticity of the coupling points. The force which is provided by the actuator will be amplified by the lever. Depending on the position where the FTE is coupled to the lever, the transmission ratio will change. If an actuator with a maximum Force of 50 N is used, a transmission ratio of about 1:4 – 1:6 is required to ensure a force of +- 100 N at the mirror substrate. With this ratio, a reduction of the step size from 20 nm to 4 nm could be possible. The sum of these single stiffnesses is represented by the stiffness that was analyzed in section II.

C. Manufacturing process

The manufacturing process, which is divided into 8 different steps, is listed in Tab. 2.

Both, the base plate and the cup shaped concave mirror substrate will be prefabricated with common technologies such as turning and milling. Inherent stress of the material will be reduced in a subsequent tempering process, by heating the components at 2/3 of the melting temperature. Additional temperature cycling causes an aging of the material, which reduces deformation of the components over time. Ultra-precision single point diamond turning is used to improve the figure of the mirror surface just before the electroless nickel plating. Nickel-Phosphorous is perfectly thermally adapted to the AlSi-composite [8] and provides sufficient hardness to achieve the extraordinary results in figure and roughness that are indispensable for the UVOIR. Figure and roughness are ensured by the turning process and alternating polishing steps. Finally, aluminium and the MgF_2 coatings will provide very high reflectance over the desired wavelength range.

Tab. 2. Manufacturing process of the DM components [9]

1	Prefabrication with common machines
2	Aging and stress relieving
3	Single Point Diamond Turning
4	Plating (electroless Nickel)
5	Single Point Diamond Turning
6	Polishing (Smoothing)
7	Polishing (Figuring)
8	Optical Coating

The transmission elements should be designed monolithically as well could be manufactured with common technologies as milling and electron discharge machining or with additive manufacturing technologies. Both, the transmission elements and the actuators will be assembled and integrated in the baseplate.

After the final manufacturing of the DM itself, it has to be fixed in all six degrees of freedom. Therefore, three bipod flexures are used. They are positioned in a 120-degree-arrangement. They allow the mirror to be mounted at its center of gravity (CG) at its neutral plane, although the bipods are not fixed at the mirror in that plane. Only imaginary lines going through the stiff axis of the flexures will cross in the neutral plane. Flexures at the end of each bipod prevent coupling of moments into the mirror. Thus, thermally induced changes of the telescope structure will not introduce significant deformations at the mirror surface [10]. Furthermore, the bipods will be made of the same aluminium alloy as the mirror body to avoid any thermal effects. Fig. 8 shows a drawing of the deformable mirror and the bipods.
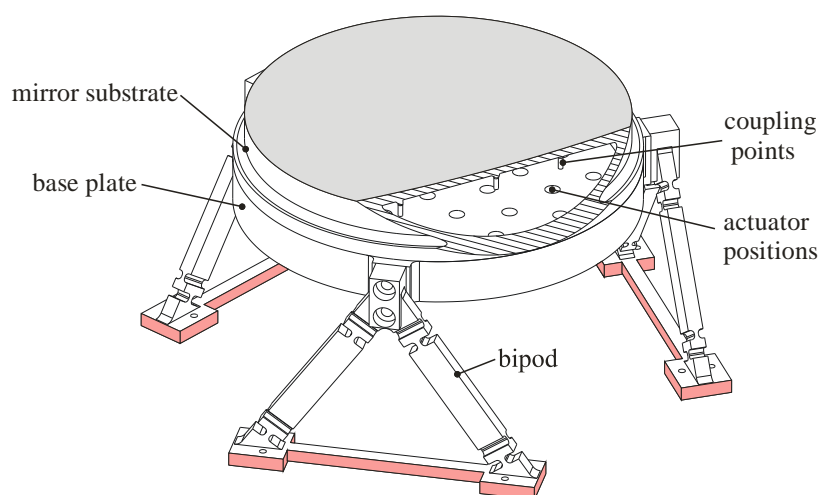

Fig. 4. Mounting concept for the deformable mirror with three bipod flexures in a 120-degree-arrangement. The red marked surfaces of the bipods are used to mount the DM with the HYPATIA telescope structure.

IV. CONCLUSIONS

We investigated the actuator layout and the actuator influence function for an active metal mirror. We figured out, that a Fibonacci distribution of 36 actuators can ensure a correction of the desired aberrations with residual RMS errors lower than 10 nm. With a variation of the actuator stiffness a residual error of 3.7 nm could be achieved. Additionally, we showed the entire simulation routine for the final design of the deformable mirror. The second part of the paper reveals the concept of the DM and how we want to manage the manufacturing of it. In summary, we could show the developing process from the requirements to the preliminary design of the DM which will be implemented in a space telescope correction chain.

ACKNOWLEDGEMENTS

REFERENCES

[1] M. Postman, T. Brown, K. Sembach, M. Giavalisco, W. Traub, K. Stapelfeldt, D. Calzetti, W. Oegerle, R. Michael Rich, P. Stahl, J. Tumlinson, M. Mountain, R. Soummer, T. Hyde, "Advanced Technology Large-Aperture Space Telescope: science drivers and technology developments", Opt. Eng., 51, 011007-011007, 2012

[2] H. P. Stahl, M. Postman, G. Mosier, W. S. Smith, C. Blaurock und K. H. a. C. C. Stark, "AMTD: update of engineering specifications derived from science requirements for future UVOIR space telescopes," Proc. SPIE 9143 Space Telescopes and Instrumentation 2014, p. 91431T, 2 August 2014.

[3] N. Devaney, C. Reinlein, N. Lange, M. Goy, A. Goncharov, & P. Hallibert, "Hypatia and STOIC: an active optics system for a large space telescope". In SPIE Astronomical Telescopes+ Instrumentation (pp. 990469-990469). International Society for Optics and Photonics, July 2016

[4] C. Reinlein, C. Damm, N. Lange, A. Kamm, M. Mohaupt, A. Brady, M. Goy, N. Leonhard, R. Eberhardt, U. Zeitner, A. Tünnermann, "Temporally-stable active precision mount for large optics," Opt. Express **24**, 13527-13541 (2016)

[5] J. Schwarz, M. Geissel, P. Rambo, J. Porter, D. Headley & M. Ramsey, "Development of a variable focal length concave mirror for on-shot thermal lens correction in rod amplifiers". Optics express, 14(23), 10957-10969, 2006

[6] G. Figueira, J. Wemans, H. Pires, N. Lopes & L. Cardoso, "Single adjuster deformable mirror with four contact points for simultaneous correction of astigmatism and defocus". Optics express, 15(9), 5664-5673, 2007

[7] R. Trines, H. Janssen, S. Paalvast, M. Teuwen, B. Brandl & M. Rodenhuis, "A cryogenic 'set-and-forget' deformable mirror". In SPIE Astronomical Telescopes+ Instrumentation (pp. 99121B-99121B). International Society for Optics and Photonics, July 2016

[8] J. Kinast, E. Hilpert, N. Lange, A. Gebhardt, R. R. Rohloff, S. Risse, ... & A. Tünnermann, "Minimizing the bimetallic bending for cryogenic metal optics based on electroless nickel". In SPIE Astronomical Telescopes+ Instrumentation (pp. 915136-915136). International Society for Optics and Photonics, July 2014

[9] R. Steinkopf, A. Gebhardt, S. Scheiding, M. Rohde, O. Stenzel, S. Gliech, V. Giggel, H. Löscher, G. Ullrich, P. Rucks, A. Duparre, S. Risse, R. Eberhardt, A. Tünnermann, "Metal mirrors with excellent figure and roughness". Proc. SPIE 7102, 71020C-71020C-12, 2008

[10] P. Yoder and D. Vukobratovich, "Opto-mechanical systems design", Fourth Edition, Volume 2: Design Analysis of Large Mirrors and Structures, Band 2, CRC Press, 2015